	Ni
14	Cr
9.5	Co
4	Mo
4	W
5	Ti
3	Al
+	C
+	Zr
+	B

RENÉ 80

1 GENERAL

René 80 is a cast, precipitation-hardenable nickel-base alloy containing chromium and cobalt with titanium and aluminum acting as the gamma-prime precipitation-hardening elements and tungsten and molybdenum added for solution strengthening. It has excellent creep-rupture strength up to 1900 F combined with good elevated temperature ductility, superior hot corrosion resistance, and good long-term stability. The latter is accomplished by selecting a balanced composition with a low electron-vacancy concentration per atom, thereby, preventing or minimizing sigma phase formation.

The alloy is difficult to machine and the usual machining methods are ECM, EDM, and low stress grinding. The only recommended joining procedures are brazing or activated diffusion bonding.

The main usage of René 80 is in investment vacuum cast turbine blades and vanes which should be coated for any long-term applications.

1.01 Commercial Designation

René 80.

1.02 Alternate Designations

1.03 Specifications

1.031 AMS specifications, none

1.032 General Electric specification C50TF28 for basic composition and mechanical properties with G.E. specifications E50TF47 and P29TF19 for electron-vacancy number and trace element control, respectively.

1.04 Composition

Composition, Table 1.04.

1.05 Heat Treatment

1.051 The preferred heat treatment is the fully heat treated condition – Class A. G. E. specification C50TF28, which is an overaging type of heat treatment for tensile ductility and low cycle fatigue capability. Tensile strength and high stress, creep-rupture capabilities are greater for the non-overage heat treatment – Class B, but this immediate advantage is lost upon exposure to high temperatures (1,4).

1.052 Various heat treated conditions, Table 1.052.

1.0521 Fully heat treated condition, Table 1.052.

1.0522 Solution treated and primary age condition, Table 1.052.

1.0523 Solution treated condition, Table 1.052.

1.06 Hardness

1.061 The hardness in the fully heat treated condition is 37 to 42 R_C (6,7).

1.062 Hardness after exposure to thermal fatigue testing in fluidized bed, Table 1.062.

1.07 Forms and Conditions Available

1.071 The alloy is available as investment vacuum castings in the as-cast or heat treated condition.

1.08 Melting and Casting Practice

1.081 Vacuum induction melting followed by vacuum casting is standard industrial practice (1). Directional solidification can result in improved mechanical properties attributed at least in part to substantially decreased casting porosity and inclusion (20). (See Figures 3.0317 and 3.045.)

1.09 Special Considerations

1.091 For long-term applications at high temperatures, the alloy should be coated to minimize oxidation and to prevent tensile embrittlement (Figure 3.0312) which can occur at strain rates encountered in conventional tensile tests conducted in air. Special coatings have been found to be effective in reducing this embrittlement. (Compare Figures 3.0314 and 3.0315.)

Coatings are also desirable to minimize deleterious effects of high temperature (1600 to 1700 F) and low temperature (1100 to 1400 F) hot corrosion in salt- and/or sulfur-containing combustion environments.

1.092 Brazing or activated diffusion bonding are the only recommended joining processes (4,9).

1.093 The recommended machining methods are EDM, ECM, and low stress grinding. Conventional or abusive grinding may have a deleterious effect on fatigue strength depending on the type of processing procedures that following the grinding operation. Aging after any type of grinding lowers the room temperature high cycle fatigue strength compared to low stress grinding of René 80 in the solution treated and aged condition. Shot peening substantially increases the room temperature high cycle fatigue strength of ground René 80 and the low cycle fatigue strength at 1400 F (4,7,10).

2 PHYSICAL AND CHEMICAL PROPERTIES

2.01 Thermal Properties

2.011 Melting range, Table 2.0111.

2.0111 Critical temperatures for six commercial VIM heats, Table 2.0111.

2.012 Phase changes, Table 2.0111.

2.0121 Time-temperature-transformation diagrams.

2.0122 The fully heat treated condition of René 80 contains approximately 47 v/o γ', 2 v/o MC (rich in titanium, tungsten and molybdenum) and very minor amounts of $M_{23}C_6$ and M_3B_2 (8).

2.0123 Effect of elevated temperature exposure on carbide stability, Figure 2.0123.

2.013 Thermal conductivity, Figure 2.013.

2.014 Thermal expansion, Figure 2.014.

2.015 Specific heat, Figure 2.015.

2.016 Thermal diffusivity.

2.02 Other Physical Properties

2.021 Density, 0.295 lb/in.^{3}, 8.17 gr/cm^3 (4).

2.022 Electrical properties.

2.023 Magnetic properties.

2.024 Emittance.

2.025 Damping capacity.

	Ni
14	Cr
9.5	Co
4	Mo
4	W
5	Ti
3	Al
+	C
+	Zr
+	B

RENÉ 80

2.03 Chemical Properties

2.031 Oxidation resistance.

2.0311 General. In dynamic oxidation tests of uncoated samples after 1000 hr at 1800 F, René 80 is inferior to René 77 and René 100, but the oxidation is more uniform, i.e., less extensive grain boundary oxidation (4,5).

2.0312 Effect of exposure in air at 1800 F on external oxidation and internal contamination, Figure 2.0312.

2.0313 Weight change during thermal fatigue testing in air in fluidized bed facility, Table 2.0313.

2.0314 Oxidation weight gain in air can be expressed by $(\Delta W/A) = Ct^{1/2}$, where ΔW = weight gain, A = area, t = time, and C = constant [in (gr/cm^2) sec 1/2], equal to 7.6×10^{-4} at 1800 F and 4.9×10^{-4} at 1700 F (23).

2.032 Hot corrosion resistance.

2.0321 General. René 80 has excellent resistance to high temperature sulfidation attack, considerably superior to René 77 and René 100, which is attributed to the high titanium-aluminum ratio (4,5).

A low temperature form of hot corrosion occurs in oil-fueled marine turbine engines. In simulated laboratory tests for 500 hr at 1250 F (10 ppm sea salt and 2 percent sulfur fuel oil), uncoated René 80 exhibited 4 mil metal loss, while coated René 80 showed <0.5 to 2 mil metal loss (24).

2.0322 Hot corrosion resistance of René 80 and other superalloys at 1600 and 1750 F, Table 2.0322.

2.04 Nuclear Environment

3 MECHANICAL PROPERTIES

3.01 Specified Mechanical Properties

3.011 Specified mechanical properties per G.E. specification C50TF28-S8, Table 3.011.

3.02 Mechanical Properties at Room Temperature

3.021 Tension–stress-strain diagrams–tension properties.

3.0211 Tension properties, Figure 3.0311.

3.022 Compression–stress-strain diagrams–compression properties.

3.023 Impact.

3.024 Bending.

3.025 Torsion and shear.

3.026 Bearing.

3.027 Stress concentration.

3.0271 Notch properties.

3.028 Combined properties.

3.03 Mechanical Properties at Various Temperatures

3.031 Tension–stress-strain diagrams–tension properties.

3.0311 Effect of room and elevated temperatures on tensile properties, Figure 3.0311.

3.0312 Effect of 1800 F exposure in air and in vacuum on the 1600 F tensile ductility of conventionally cast and directionally solidified René 80, Figure 3.0312.

3.0313 Effect of surface removal on the 1600 F tensile ductility of specimens exposed in air at 1650, 1700, and 1800 F, Figure 3.0313.

3.0314 Effect of testing atmosphere and strain rate on the 1600 F tensile ductility of specimens exposed in vacuum at 1800 F, Figure 3.0314.

3.0315 Effect of various protective coatings and strain rate on the 1600 F tensile ductility of coated specimens exposed in air at 1800 F, Figure 3.0315.

3.0316 Effect of coatings on tensile properties at 1400 to 1800 F, Figure 3.0316.

3.0317. Effect of directional solidification on room and elevated temperature tensile properties, Figure 3.0317.

3.032 Compression–stress-strain–compression properties.

3.033 Impact.

3.034 Bending.

3.035 Torsion and shear.

3.036 Bearing.

3.037 Stress concentration.

3.0371 Notch properties.

3.0372 Fracture toughness.

3.038 Combined properties.

3.04 Creep and Creep-Rupture Properties

3.041 Creep-strain and creep-rupture curves at 1400, 1600, and 1800 F for fully heat treated cast alloy, Figure 3.041.

3.042 Creep-strain and creep-rupture curves at 1500, 1700, 1900, and 2000 F for fully heat treated cast alloy, Figure 3.042.

3.043 Stress rupture ductility at 1400 to 1900 F, Table 3.043.

3.044 Effect of coatings on rupture life at 1400, 1600, and 1800 F, Figure 3.044.

3.045 Effect of directional solidification on rupture life at 1400, 1600, and 1800 F, Figure 3.045.

3.05 Fatigue Properties

3.051 High cycle fatigue.

3.0511 Effect of surface grinding procedures on the high cycle fatigue life at room temperature, Figure 3.0511.

3.0512 Effect of various ECM and EDM procedures on the high cycle fatigue life at room temperature, Figure 3.0512.

3.052 Low cycle fatigue.

3.0521 Effect of surface grinding and EDM procedures on the 1400 F low cycle fatigue life, Figure 3.0521.

3.0522 Effect of ECM plus shot peening on the 1400 F low cycle fatigue life, Figure 3.0522.

3.0523 General. The effects of various surface grinding, ECM, and EDM procedures on high and low cycle fatigue life can be significantly affected by post-processing operations, such as solution and/or aging heat treatments, diffusion coating temperatures, the removal of cold-worked surface layers by pickling, shot peening, and residual stresses. See Reference 7, pp. 237-281 for details.

3.0524 Axial low cycle fatigue behavior at 1200 to 1800 F, Figure 3.0524.

3.0525 Effect of combined plastic and creep-strain cycles on low cycle fatigue life at 1832 F in high vacuum, Figure 3.0525. [Similar tests were conducted at 1600 F with nearly identical results (27).]

3.0526 Effect of combined plastic and creep-strain cycles on low cycle fatigue life at 1832 F in air, Figure 3.0526.

3.0527 Comparison of hold time experiments with frequency modified fatigue equation representation of continuous cycling experiments at 1600 F, Figure 3.0527.

3.0528 Effect of hold period and wave shape on low cycle fatigue life at 1600 F, Figure 3.0528.

3.0529 Effect of strain rate and hold time on low cycle fatigue life at 1600 and 1800 F, Figure 3.0529.

3.0530 Effect of prior air exposure and cycle frequency on low cycle fatigue life at 1600 F, Figure 3.0530.

3.0531 Effect of strain rate and hold time on low cycle fatigue life of notched specimens at 1400 and 1800 F, Figure 3.0531.

3.0532 Cyclic stress-strain curves at 1600 and 1832 F in air and vacuum, Figure 3.0532.

3.054 Thermal fatigue.

3.0541 Thermal cycles required to initiate first crack in each edge of double edge wedge specimen in fluidized bed testing, Table 3.0541.

3.0542 General. By using activated diffusion bonding to join a monocrystalline edge of René 80 to conventionally cast polycrystalline airfoils, the thermal fatigue life of such composites has been increased four to eight fold compared to conventionally cast René 80 blades (15,16).

3.06 Elastic Properties

3.061 Poisson's ratio, Figure 3.061.

3.062 Modulus of elasticity, Figure 3.062.

3.0621 Dynamic modulus of elasticity at room temperature = 29.9×10^6 psi (18).

3.063 Modulus of rigidity.

3.064 Tangent modulus.

3.065 Secant modulus.

4 FABRICATION

4.01 Forming

4.011 Hot isostatic pressing can improve the room temperature fatigue strength and stress rupture strength (approximately 30 percent) of castings containing excessive as-cast porosity. However, porosity-free castings are unaffected by the HIP process (19).

4.02 Machining and Grinding

4.021 René 80 is difficult to machine. The usual machining methods are ECM, EDM, and low stress grinding (4).

4.022 Low stress grinding should be used in place of conventional grinding to minimize distortion and reduce the possibility of producing extensive metallurgical changes or cracking in the surface layer. Low stress grinding (LSG) is accomplished by using softer grinding wheels, reduced wheel speeds and infeed rates, and more chemically active cutting fluids than those employed in conventional grinding. LSG should be used particularly for removing the last 0.010 inch of material with stock removal on the order of 0.0005 to 0.0002 inch per pass. See Reference 10, pp. 20-26 for details.

4.023 When EDM or EDG is used, the recast or heat-affected layer that is produced should be removed, since it lowers the fatigue strength. See Reference 10, pp. 31-34 for details.

4.024 Steel shot peening can be used to restore or enhance the normal fatigue characteristics of René 80 (7,10).

4.03 Joining

4.031 Brazing or activated diffusion bonding in vacuum are the only recommended joining procedures. The latter process produces joints with the highest strengths (4,9).

4.032 Tensile properties at elevated temperatures of activated diffusion bonded butt joints versus base metal, Figure 4.032.

4.033 Stress rupture strength of activated diffusion bonded butt joints versus brazed joints versus base metal, Figure 4.033.

4.034 High cycle fatigue strength of activated diffusion bonded butt joints versus base metal at 1400 F, Figure 4.034.

4.035 High joint strengths can be produced by activated diffusion bonding with joint gap variations ranging from 0.0005 to 0.010 inch (9).

4.036 René 80 has been successfully joined to TDNiCr and U-700 by activated diffusion bonding. Extensive mechanical properties data on overlap and butt joints of such composites are reported in Reference 17.

Activated diffusion bonded butt joints of René 80 to single crystal Normalloy have also been made successfully, with property data on bonded specimens given in Reference 31.

4.04 Surface Treating

4.041 Shot peening (see Section 4.024).

4.042 Protective diffusion-type coatings are recommended to improve oxidation resistance for long-term applications and to prevent tensile embrittlement (4,8).

4.043 Suitable protective coatings when sufficiently thick and ductile to sustain and confine surface cracking under conventional tensile testing strain rates can reduce hot tensile embrittlement which has been shown to be environmentally related. Tensile embrittlement is caused by interactions of nitrogen and probably also oxygen with the grain-boundary γ' network which occurs upon exposure to air. (Compare Figures 3.0314 and 3.0315.)

	Ni
14	Cr
9.5	Co
4	Mo
4	W
5	Ti
3	Al
+	C
+	Zr
+	B

RENÉ 80

REFERENCES

1 G.E. Specification C50TF28-S8 (July 2, 1975).

2 G.E. Specification E50TF47-S4 (November 13, 1972).

3 G.E. Specification P29TF19-S5 (December 10, 1973).

4 Materials Handbook, Section 2-Metallic Materials, Ni-Base, René 80, Flight Propulsion Division, General Electric Company, Cincinnati, Ohio (1970-1973 incl.).

5 Ross, Earl W., "René 80: A Cast Turbine Blade Alloy", Metal Progress, Vol. 99, No. 3 (March 1971) pp. 93-94.

6 Howe, M.A.H., "Additional Thermal Fatigue Data on Nickel- and Cobalt-Base Superalloys", Final Report (Part 2), IIT Research Institute, Chicago, Illinois, NASA CR-121212, IITRI-B6107-34 (March 15, 1973).

	Ni
14	Cr
9.5	Co
4	Mo
4	W
5	Ti
3	Al
+	C
+	Zr
+	B

RENÉ 80

7 Koster, W. P., "Surface Integrity of Machine Materials", Metcut Research Associates Inc., Technical Report AFML-TR-74-60 (April 1974).

8 Chang, W. H., "Tensile Embrittlement of Turbine Blade Alloys After High Temperature Exposure", General Electric Company, Cincinnati, Ohio, MCIC Report 72-10 (September 1972).

9 Hoppin, G. S., III, and Berry, T. F., "Activated Diffusion Bonding", General Electric Company, Cincinnati, Ohio, Welding Research Supplement (November 1970).

10 Koster, W. P., "Manufacturing Methods for Surface Integrity of Machined Structural Components", Metcut Research Associates Inc., Technical Report AFML-TR-71-258 (April 1972).

11 Howes, M.A.H., "Additional Thermal Fatigue Data on Nickel- and Cobalt-Base Superalloys", Final Report (Part 1), IIT Research Institute, Chicago, Illinois, NASA CR-121211, IITRI-B6107-34 (March 15, 1973).

12 Lord, D. C., and Coffin, L. F., Jr., "Low Cycle Fatigue Hold Time Behavior of Cast René 80", Metallurgical Transactions, Vol. 4, No. 7 (July 1973) p. 1647-54.

13 Coffin, L. F., Jr., "Proceedings Air Force Conference on Fatigue and Fracture of Aircraft Structures and Materials", AFFDL TR 70-144 (1970) p. 301-312.

14 Coffin, L. F., Jr., General Electric Company, Schenectady, New York, Unpublished Research (1973).

15 Semmel, J. W., Berry, T. F., and Zelahy, J. W., "Fabricated Turbine Blade with Monocrystal Edge", General Electric Company, paper presented at the Third Air Force Metalworking Conference, Los Angeles, California (March 13-17, 1972).

16 Simmons, Ward F., "Current and Future Materials Usage in Aircraft Gas Turbine Engines", Battelle's Columbus Laboratories, MCIC Report 73-14 (June 1973).

17 Wilbers, L. G., Berry, T. F., Kutchera, R. E., and Edmonson, R. E., "Development of the Activated Diffusion Brazing Process for Fabrication of Finned Shell to Strut Turbine Blades", General Electric Company, Cincinnati, Ohio, NASA Lewis Contract NAS3-12433, NASA CR-72-844 (November 1971).

18 Bion, P. T., and Spera, D. A., "Comparative Thermal Fatigue Resistances of Twenty-Six Ni- and Co-Base Alloys", NASA Lewis Research Center, Cleveland, Ohio, NASA TN D-8071 (October 1975).

19 Bailey, P. G., and Lowe, D. H., "Process for High Integrity Castings", General Electric Company, Cincinnati, Ohio, Report AFML-TR-74-152 (July 1974).

20 Nakagawa, Y. G., Ohtomo, A., and Saiga, Y., "Directional Solidification of René 80", Transactions of the Japan Institute of Metals, Vol. 17, No. 6 (June 1976) p. 323-329.

21 Semchyshen, M., "Processing: The Rediscovered Dimension in High Temperature Alloys", ASTM Standardization News, Vol. 4, No. 4 (April 1976) p. 9-19.

22 McKnight, R. L., Laflen, J. H., and Spamer, G. T., "Turbine Blade Tip Durability Analysis", General Electric Company, Cincinnati, Ohio, NASA CR-165268 (February 1981).

23 Antolovich, S. D., Liu, S., and Baur, R., "Low Cycle Fatigue Behavior of René 80 at Elevated Temperature", Metallurgical Transactions, Vol. 12A, No. 3 (March 1981) p. 473-481.

24 Eppinger, E. V., Halnan, W. K., and Boone, D. H., "Hot Corrosion Evaluation of Co-Cr-Al Coatings Modified by Active Elements", Thin Solid Films, Vol. 73, No.2 (November 17, 1980) p. 415-417.

25 Fritz, L. J., and Koster, W. P., "Tensile and Creep Properties of (16) Uncoated and (2) Coated Engineering Alloys at Elevated Tempratures", Metcut Research Associates Inc., Cincinnati, Ohio, NAS CR-135138 (January 15, 1977).

26 Sheinker, A. A., "Exploratory Thermal-Mechanical Fatigue Results for René 80 in Ultrahigh Vacuum", TRW Inc., Cleveland, Ohio, NASA CR-159444 (October 1978).

27 Kortovich, C. S., "Ultrahigh Vacuum, High Temperature, Low Cycle Fatigue of Coated and Uncoated René 80", TRW Inc., Cleveland, Ohio, NASA CR-135003 (April 1976).

28 Shockley, Q. O., Hodshire, J. O., and Pacala, T., "Exploratory Development of an Overhaul Coating Process for Gas Turbine Components", Detroit Diesel Allison Division of General Motors Corp., Indianapolis, Indiana, AFML-TR-78-84 (June 1978).

29 Halford, G. R., and Nachtigall, A. J., "Strainrange Partitioning Behavior of the Nickel-Base Superalloys, René 80 and IN 100", NASA Lewis Research Center, NASA TM-78828, presented at AGARD Specialists' Meeting, Aalborg, Denmark (April 9-14, 1978).

30 Antolovich, S. D., "Microstructural Effects and Fatigue Life Predictions of Notched and Un-Notched Ni Base Superalloys at Elevated Temperatures", University of Cincinnati, Ohio, AFOSR TR-80-0341 (April 1980).

31 Zelahy, J. W., and Fairbanks, N. P., "Advanced Turbine Blade Tip Seal System – Volume I", General Electric Company, Cincinnati, Ohio, NASA CR-167851 (July 1982).

BIBLIOGRAPHY

1 Coffin, L. F., Jr., "The Effect of Frequency on the Cyclic Strain and Fatigue Behavior of Cast René 80 at 1600 F", Metallurgical Transactions, Vol. 5, No. 1, p. 1053-1060 (May 1974).

2 Collins, H. E., "The Effect of Thermal Exposure on the Microstructure and Mechanical Properties of Nickel-Base Superalloys", Metallurgical Transactions, Vol. 5, No. 1, p. 189-204 (January 1974).

3 Kaufman, M., "Examination of the Influence of Coatings on Thin Superalloy Sections", Vol. 1, Description and Analysis, General Electric Company, Cincinnati, Ohio, Report NASA CR-134791 (December 1974).

4 Ibid, Vol. 2, Detailed Procedures and Data, Report NASA CR-134792 (December 1974).

Alloy	René 80	
	Percent	
Composition	Min	Max
C	0.15	0.19
Mn	–	0.10
Si	–	0.10
S	–	0.0075
P	–	0.015
Cr	13.70	14.30
Co	9.00	10.00
Ti	4.80	5.20
Al	2.80	3.20
Mo	3.70	4.30
W	3.70	4.30
Mo + W	7.70	–
B	0.01	0.02
Zr	0.02	0.10
Fe	–	0.35
Cb	–	0.10
Ta	–	0.10
V	–	0.10
Cu	–	0.10
Hf	–	0.10
Mg	–	0.01
Ni	Balance	

$\bar{N}_{V3}$ shall be 2.32 maximum electron vacancy number calculated by the method described in G.E. specification E50TF47 (2).

Trace element content shall meet the requirements of G.E. specification P29TF19 (3) and be applicable to turbine blades only.

TABLE 1.04. COMPOSITION (1)

Ni
14 Cr
9.5 Co
4 Mo
4 W
5 Ti
3 Al
+ C
+ Zr
+ B

RENÉ 80

Alloy	René 80		
Condition	Fully Heat Treated	Solution Treated and Primary Age	Solution Treated Only
G.E. Specification C50TF28	Class A	Class B	Class D
Step 1	2175 to 2225 F, 2 hr in Vacuum; Furnace Cool in Vacuum, Ar or He to 1975 to 2025 F within 10 min (a,b)	Same	Same
Step 2	Hold at 1975 to 2025 F, 4 hr in Vacuum; Furnace Cool to 1200 F in Vacuum, Ar or He within 60 min; Hold at 1200 F, 10 min	Same	(c)
Step 3	Raise Temp to 1925 F and Hold at 1900 to 1950 F, 2 to 12 hr in Vacuum, Ar or He; Cool to 1200 F within the Range of 15 to 60 min and Hold at 1200 F for 10 min (d)	Furnace or AC to Room Temp	–
Step 4	Raise Temp to 1550 F and Hold at 1525 to 1575 F, 16 hr in Vacuum, Ar or He; Furnace or AC to Room Temp	–	–

(a) Cooling to 1200 F within 60 minutes is optional.
(b) Cooling to room temperature is optional.
(c) Continue furnace cool to 1200 F in vacuum, argon, or helium within 60 minutes; furnace or AC to room temperature.
(d) When parts are coated, Step 3 is omitted.

TABLE 1.052. VARIOUS HEAT TREATED CONDITIONS (1,4,5)

	Ni
14	Cr
9.5	Co
4	Mo
4	W
5	Ti
3	Al
+	C
+	Zr
+	B

RENÉ 80

Alloy	René 80			
Condition[a]	Fully Heat Treated (Original Hardness R_C 42) Hardness R_C After Exposure			
Cycles	50	100	200	500
Thermal Cycle[b]				
2065/675 F	–	38	–	–
1990/600 F	–	–	–	41
1915/525 F	40	–	38	37

(a) C50TF28, Class A: 2200 F + 2000 F + 1925 F + 1550 F.
(b) Dwell for 3 minutes in each bed at the Fluidized Bed Thermal Fatigue Test Facility at IITRI.

TABLE 1.062. HARDNESS AFTER EXPOSURE TO THERMAL FATIGUE TESTING IN FLUIDIZED BED (6)

Alloy	René 80
	Temperature, F[a]
Liquidus	2403 to 2414
Start of MC Formation	2367 to 2374
Solidus	2324 to 2341
Start of γ-γ' Eutectic Formation	2196 to 2205
γ' Solvus	2101 to 2120

(a) Determined by differential thermal analysis.

TABLE 2.0111. CRITICAL TEMPERATURES FOR SIX COMMERCIAL VIM HEATS (21)

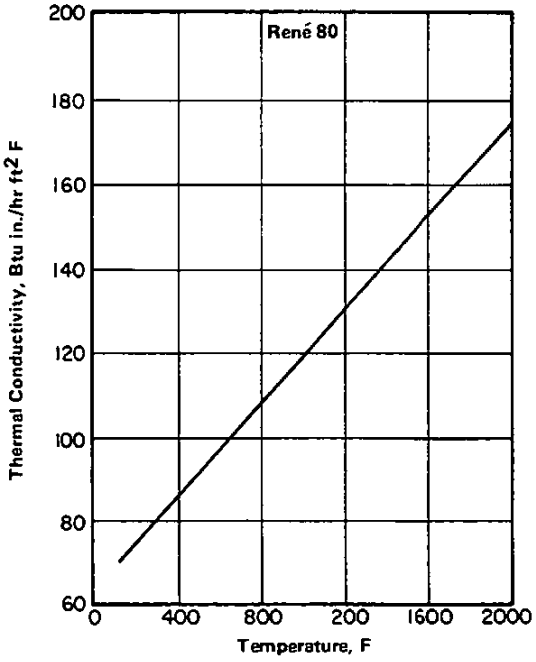

FIGURE 2.013. THERMAL CONDUCTIVITY (4)

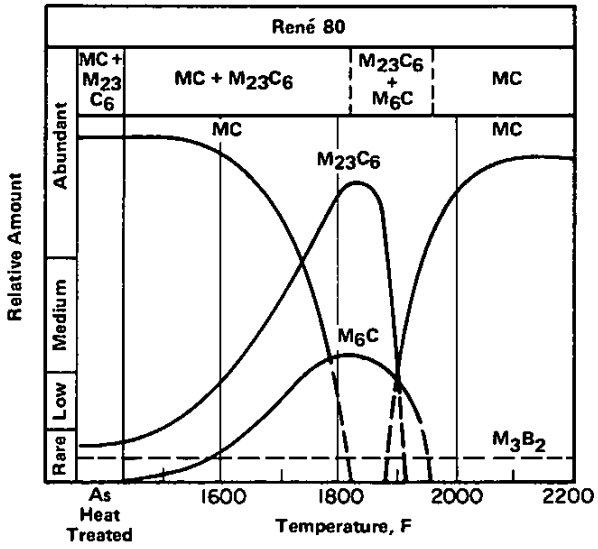

FIGURE 2.0123. EFFECT OF ELEVATED TEMPERATURE EXPOSURE ON CARBIDE STABILITY (8)

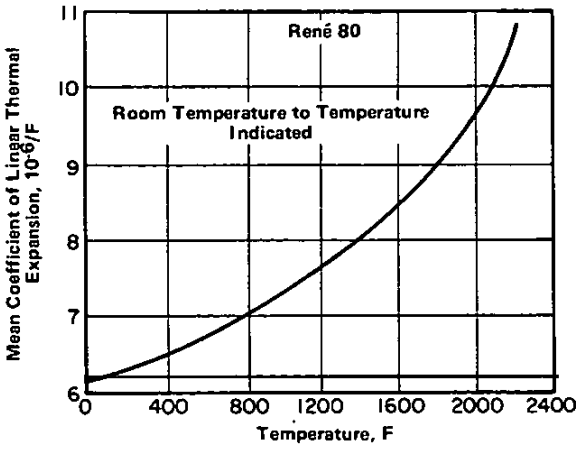

FIGURE 2.014. THERMAL EXPANSION (22)

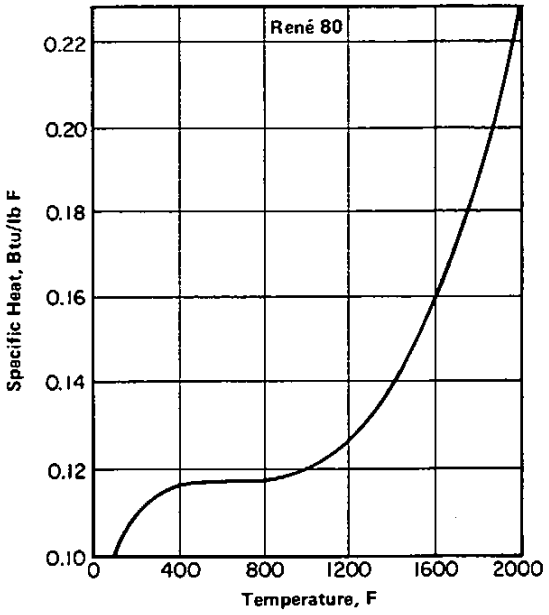

FIGURE 2.015. SPECIFIC HEAT (4)

Alloy	René 80			
Cycles	50	100	200	500
	Weight Change, percent			
Thermal Cycle[a]				
2065/675 F	–	+0.06	-0.08	–
1990/600 F	–	–	–	-0.25
1915/525 F	+0.07	–	+0.08	-0.28

(a) Uncoated samples dwelled for 3 minutes in each bed at Fluidized Bed Thermal Fatigue Test Facility: original specimen weight is 117 to 125 gr.; air flow for 3 minutes measured at 150 F, 2 psi pressure: hot bed is 900 cfh: intermediate bed is 2100 cfh.

TABLE 2.0313. WEIGHT CHANGE DURING THERMAL FATIGUE TESTING IN AIR IN FLUIDIZED BED FACILITY (1)

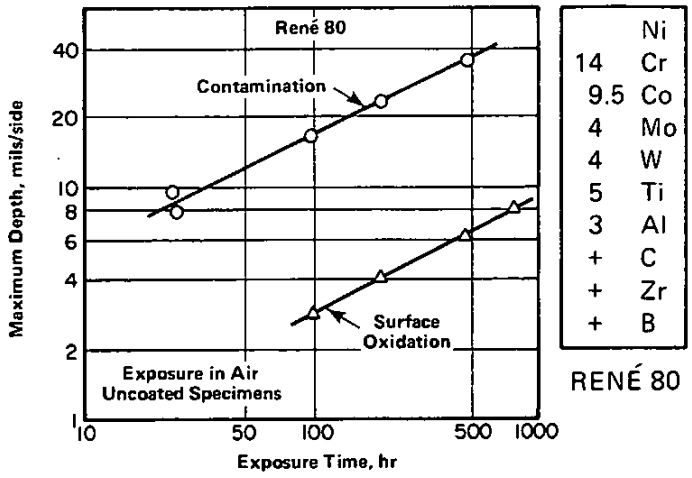

FIGURE 2.0312. EFFECT OF EXPOSURE IN AIR AT 1800 F ON EXTERNAL OXIDATION AND INTERNAL CONTAMINATION (8)

Alloy	René 80					
Test Temp, F	1600			1750		
Depth of Attack, mils per side	a	b	c	a	b	c
Alloy						
René 80	3.9	10.2	12.2	2.5	7.9	8.9
René 77	35.3	43.5	47.4	25.9	36.0	43.8
Inconel 713		65+		29.9	36.0	39.0
René 100		65+			65+	

Note: a = surface loss; b = average penetration; and c = maximum penetration after 1,000 hr at temperature at 5 ppm ingested salt. Laboratory test was at low velocity; hot blast test was performed using jet fuel at the G.E. Lynn testing facility.

TABLE 2.0322. HOT CORROSION RESISTANCE OF RENÉ 80 AND OTHER SUPERALLOYS AT 1600 AND 1750 F

Alloy	René 80	
Form	Cast to Size or Cast Machined Specimens	
Condition	Fully Heat Treated – Class A[a]	
Test Temp, F	1600	1800
F_{tu}, ksi (Min)	90	–
F_{ty}, ksi (Min)	70	–
RA, percent (Min)	15	–
Stress Rupture – 27.5 ksi		
hr (Min)	–	23
RA, percent (Min)	–	5

(a) See Table 1.052.

Note: Tensile tests per ASTM E21. For referee tensile tests, use $\dot{e}$ or 0.005 per minute thru F_{ty}.

TABLE 3.011. SPECIFIED MECHANICAL PROPERTIES PER G.E. SPECIFICATION C50TF28-S8 (1)

	Ni
14	Cr
9.5	Co
4	Mo
4	W
5	Ti
3	Al
+	C
+	Zr
+	B

RENÉ 80

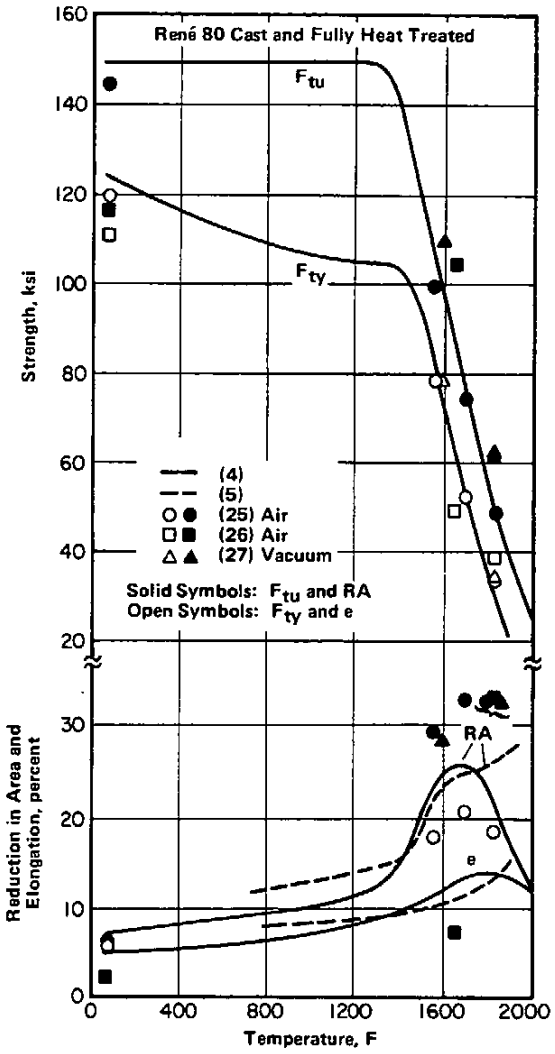

FIGURE 3.0311. EFFECT OF ROOM AND ELEVATED TEMPERATURE ON TENSILE PROPERTIES (4,5,25-27)

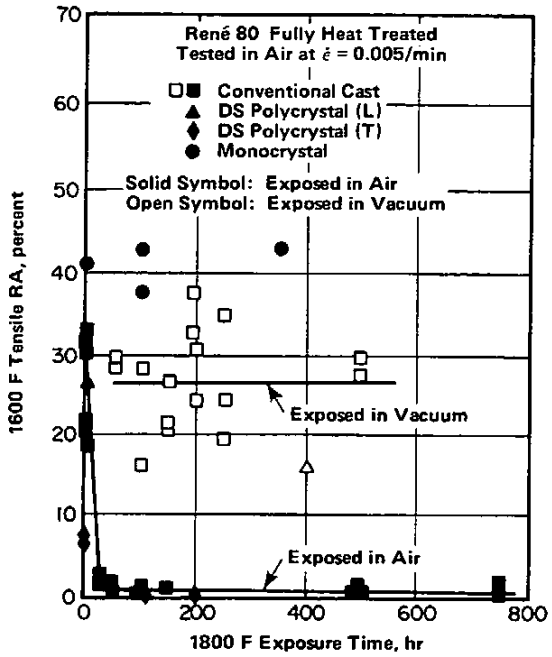

FIGURE 3.0312. EFFECT OF 1800 F EXPOSURE IN AIR AND IN VACUUM ON THE 1600 F TENSILE DUCTILITY OF CONVENTIONALLY CAST AND DIRECTIONALLY SOLIDIFIED RENÉ 80 (8)

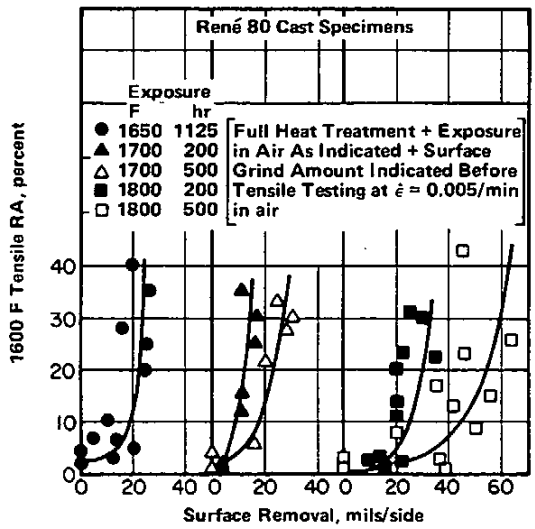

FIGURE 3.0313. EFFECT OF SURFACE REMOVAL ON THE 1600 F TENSILE DUCTILITY OF SPECIMENS EXPOSED IN AIR AT 1650, 1700, AND 1800 F (8)

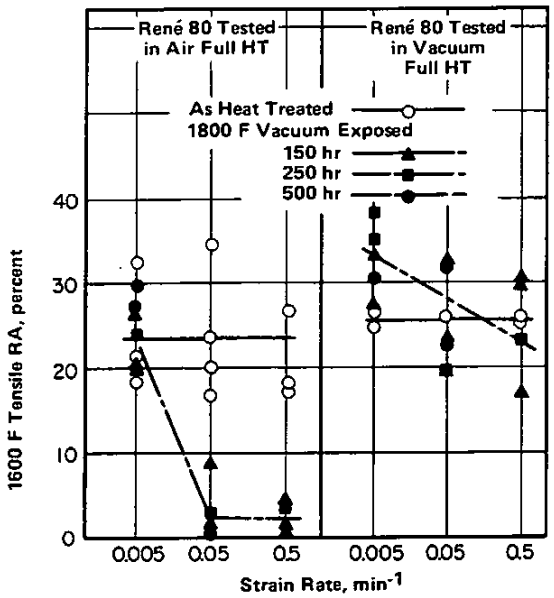

	Ni
14	Cr
9.5	Co
4	Mo
4	W
5	Ti
3	Al
+	C
+	Zr
+	B

RENÉ 80

FIGURE 3.0314. EFFECT OF TESTING ATMOSPHERE AND STRAIN RATE ON THE 1600 F TENSILE DUCTILITY OF SPECIMENS EXPOSED IN VACUUM AT 1800 F (8)

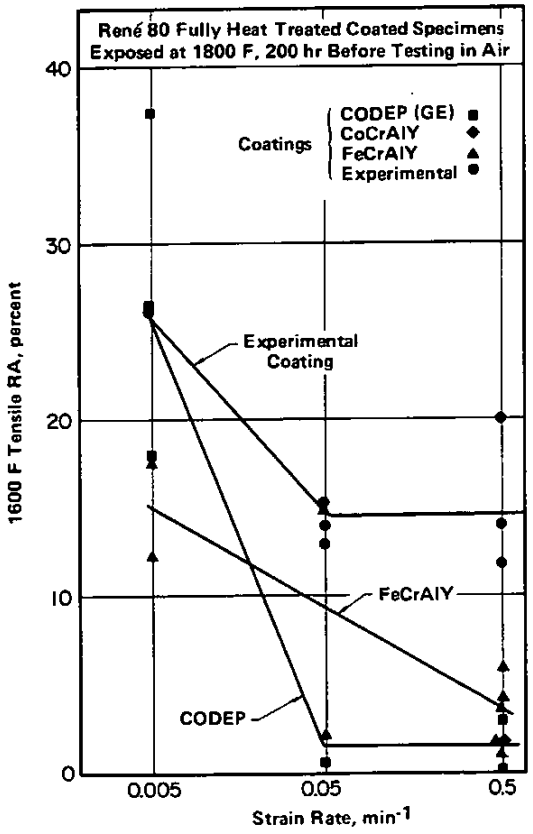

FIGURE 3.0315. EFFECT OF VARIOUS PROTECTIVE COATINGS AND STRAIN RATE ON THE 1600 F TENSILE DUCTILITY OF COATED SPECIMENS EXPOSED IN AIR AT 1800 F (8)

	Ni
14	Cr
9.5	Co
4	Mo
4	W
5	Ti
3	Al
+	C
+	Zr
+	B

RENÉ 80

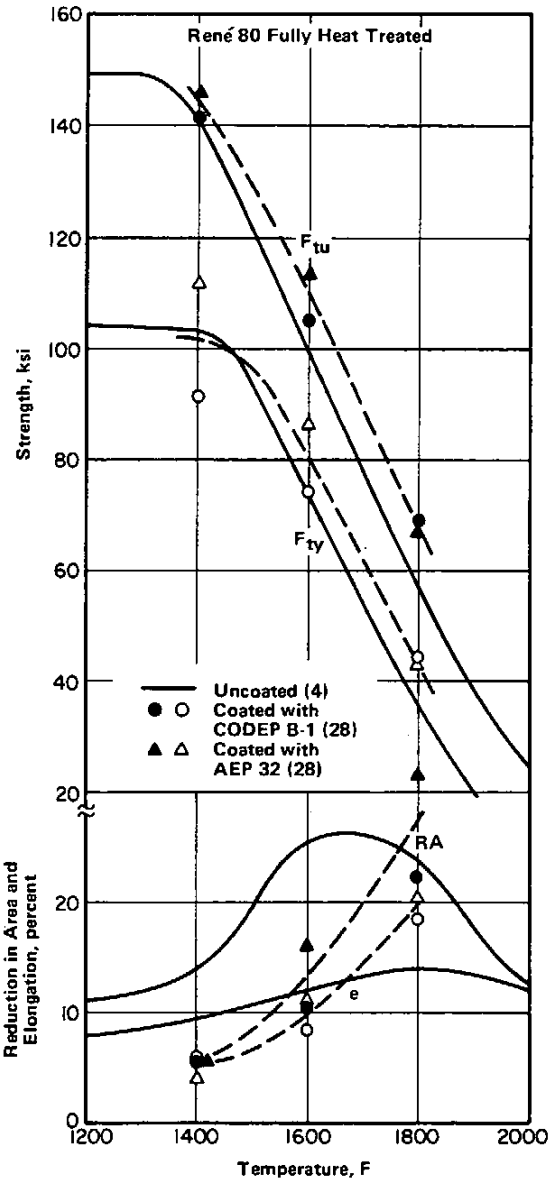

FIGURE 3.0316. EFFECT OF COATINGS ON TENSILE PROPERTIES AT 1400 TO 1800 F (4,28)

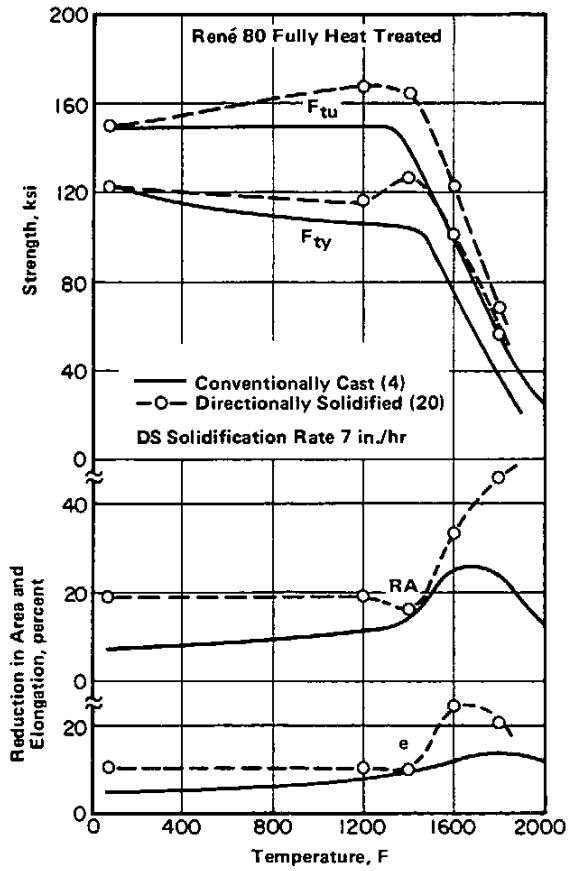

FIGURE 3.0317. EFFECT OF DIRECTIONAL SOLIDIFICATION ON ROOM AND ELEVATED TEMPERATURE TENSILE PROPERTIES (4,20)

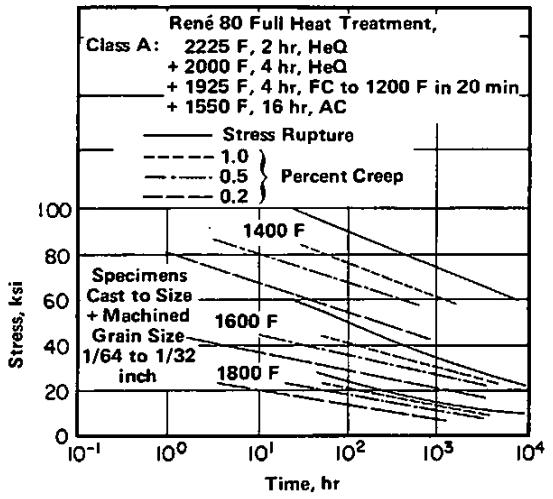

FIGURE 3.041. CREEP-STRAIN AND CREEP-RUPTURE CURVES AT 1400, 1600, AND 1800 F FOR FULLY HEAT TREATED CAST ALLOY (4)

	Ni
14	Cr
9.5	Co
4	Mo
4	W
5	Ti
3	Al
+	C
+	Zr
+	B

RENÉ 80

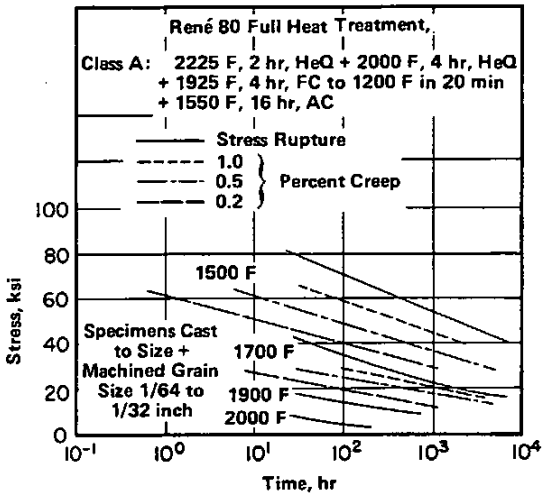

FIGURE 3.042. CREEP-STRAIN AND CREEP-RUPTURE CURVES AT 1500, 1700, 1900, AND 2000 F FOR FULLY HEAT TREATED CAST ALLOY (4)

Alloy	René 80					
Form(a)	Investment Vacuum Cast					
Condition(b)	Fully Heat Treated – Class A					
Test Temp, F	1400	1500	1600	1700	1800	1900
e, percent (Avg)						
100 hr	9.7	7.9	6.9	6.0	5.2	4.6
1,000 hr	6.6	6.2	5.9	5.6	5.4	5.2
10,000 hr	7.6	8.1	8.5	9.0	9.4	9.8
RA, percent (Avg)						
100 hr	17.8	14.9	12.5	10.5	8.8	7.4
1,000 hr	12.9	10.6	8.7	7.2	5.9	4.9
10,000 hr	9.3	7.5	6.1	4.9	4.0	3.2

(a) Specimens were cast to size, then machined; grain size is 1/64 to 1/32 inch.
(b) Heat treatment: 2225 F, 2 hr, HeQ
+2000 F, 4 hr, HeQ
+1925 F, 4 hr, FC to 1200 F in 20 min, AC
+1550 F, 16 hr, AC

TABLE 3.043. STRESS RUPTURE DUCTILITY AT 1400 TO 1900 F (4)

	Ni
14	Cr
9.5	Co
4	Mo
4	W
5	Ti
3	Al
+	C
+	Zr
+	B

RENÉ 80

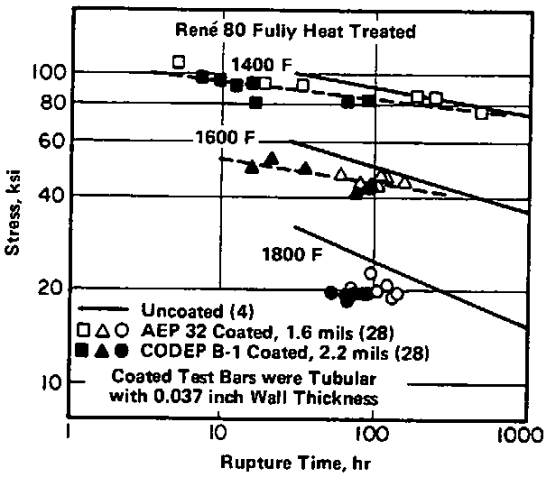

FIGURE 3.044. EFFECT OF COATINGS ON RUPTURE LIFE AT 1400, 1600, AND 1800 F (4,28)

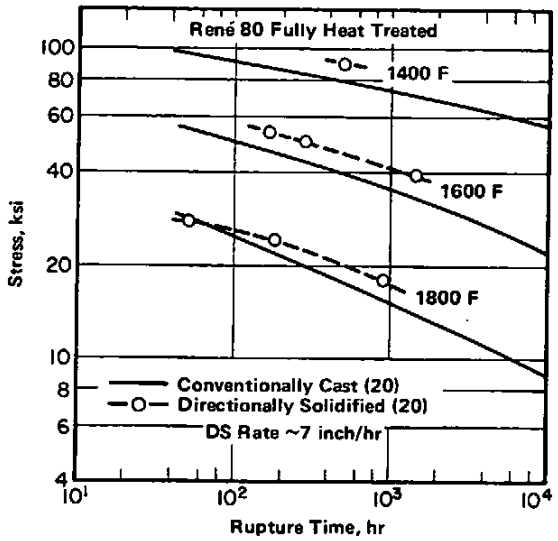

FIGURE 3.045. EFFECT OF DIRECTIONAL SOLIDIFICATION (DS) ON RUPTURE LIFE AT 1400, 1600, AND 1800 F (20)

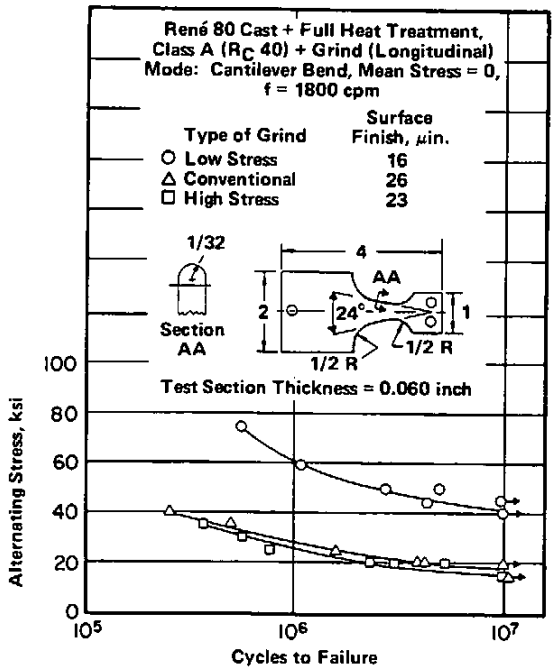

FIGURE 3.0511. EFFECT OF SURFACE GRINDING PROCEDURES ON THE HIGH CYCLE FATIGUE LIFE AT ROOM TEMPERATURE (10)

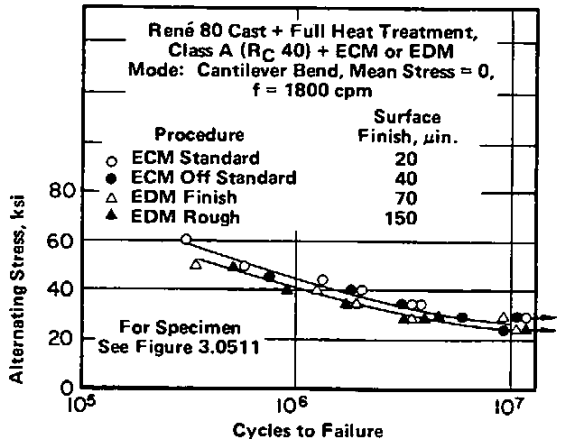

FIGURE 3.0512. EFFECT OF VARIOUS ECM AND EDM PROCEDURES ON THE HIGH CYCLE FATIGUE LIFE AT ROOM TEMPERATURE (10)

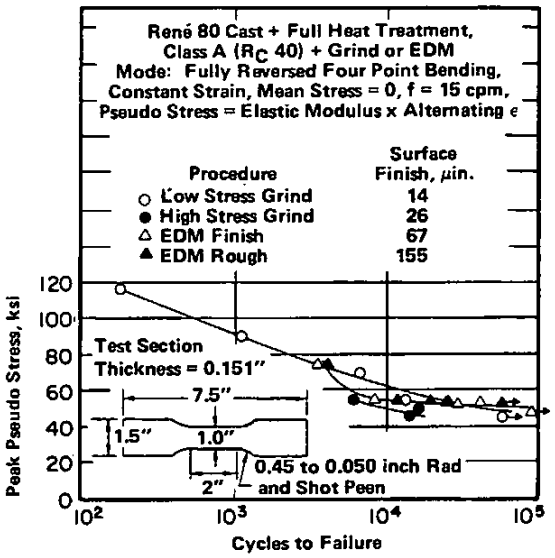

FIGURE 3.0521. EFFECT OF SURFACE GRINDING AND EDM PROCEDURES ON THE 1400 F LOW CYCLE FATIGUE LIFE (10)

	Ni
14	Cr
9.5	Co
4	Mo
4	W
5	Ti
3	Al
+	C
+	Zr
+	B

RENÉ 80

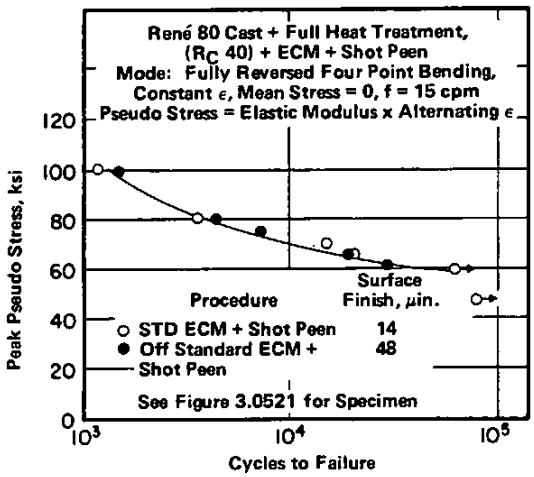

FIGURE 3.0522. EFFECT OF ECM PLUS HOT PEENING ON THE 1400 F LOW CYCLE FATIGUE LIFE (10)

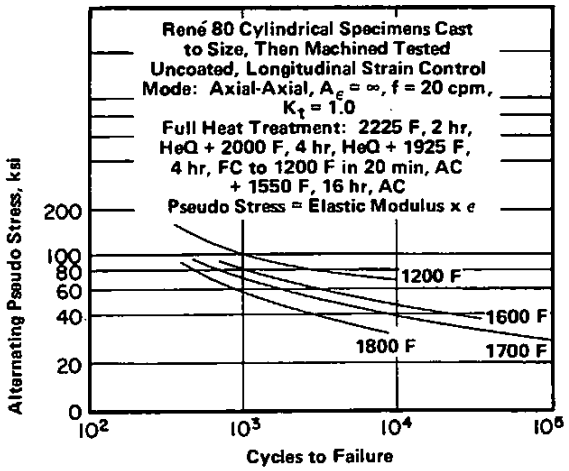

FIGURE 3.0524. AXIAL LOW CYCLE FATIGUE BEHAVIOR AT 1200 TO 1800 F (4)

	Ni
14	Cr
9.5	Co
4	Mo
4	W
5	Ti
3	Al
+	C
+	Zr
+	B

RENÉ 80

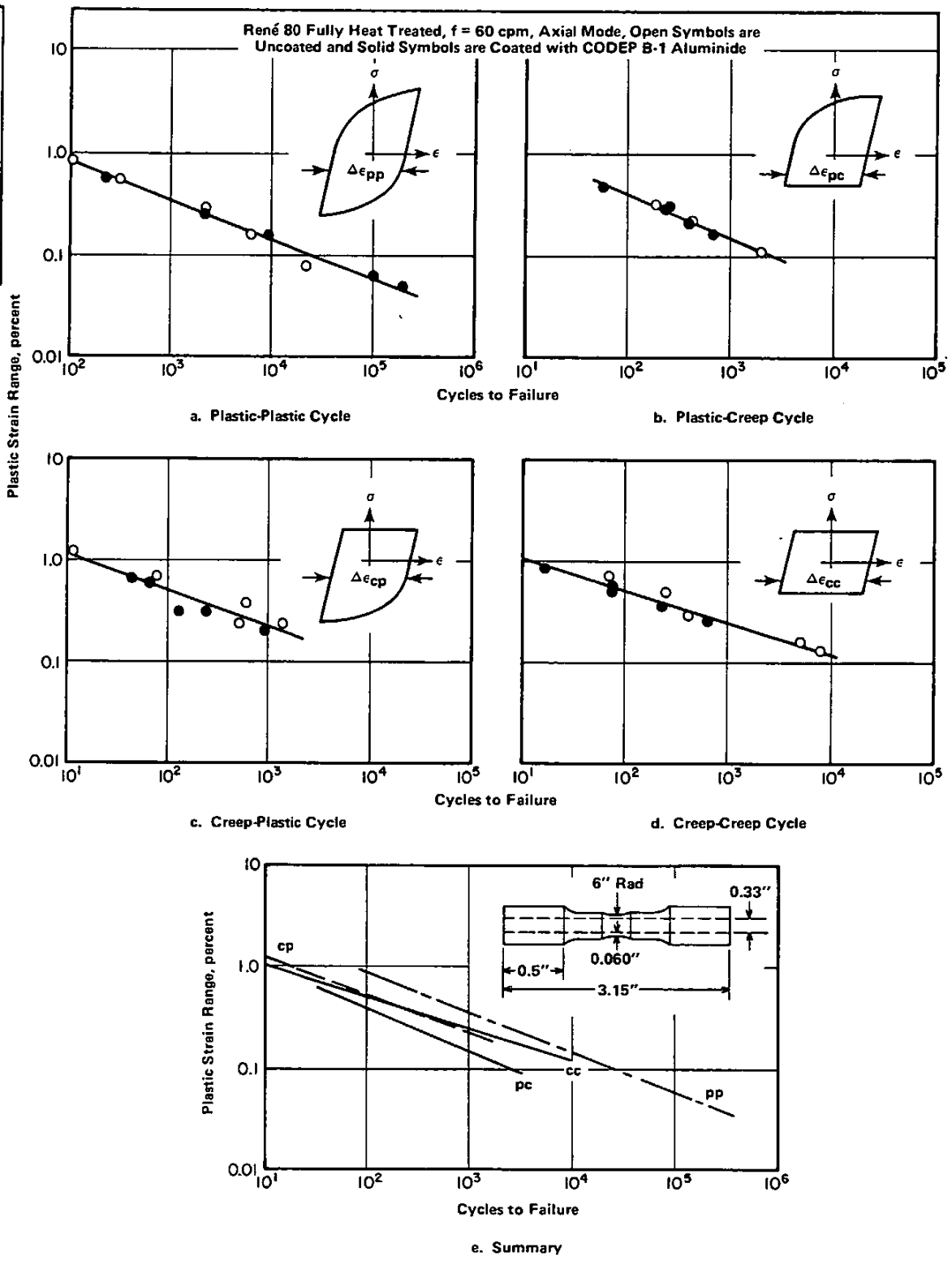

FIGURE 3.0525. EFFECT OF COMBINED PLASTIC AND CREEP-STRAIN CYCLES ON LOW CYCLE FATIGUE LIFE AT 1832 F IN HIGH VACUUM (27)

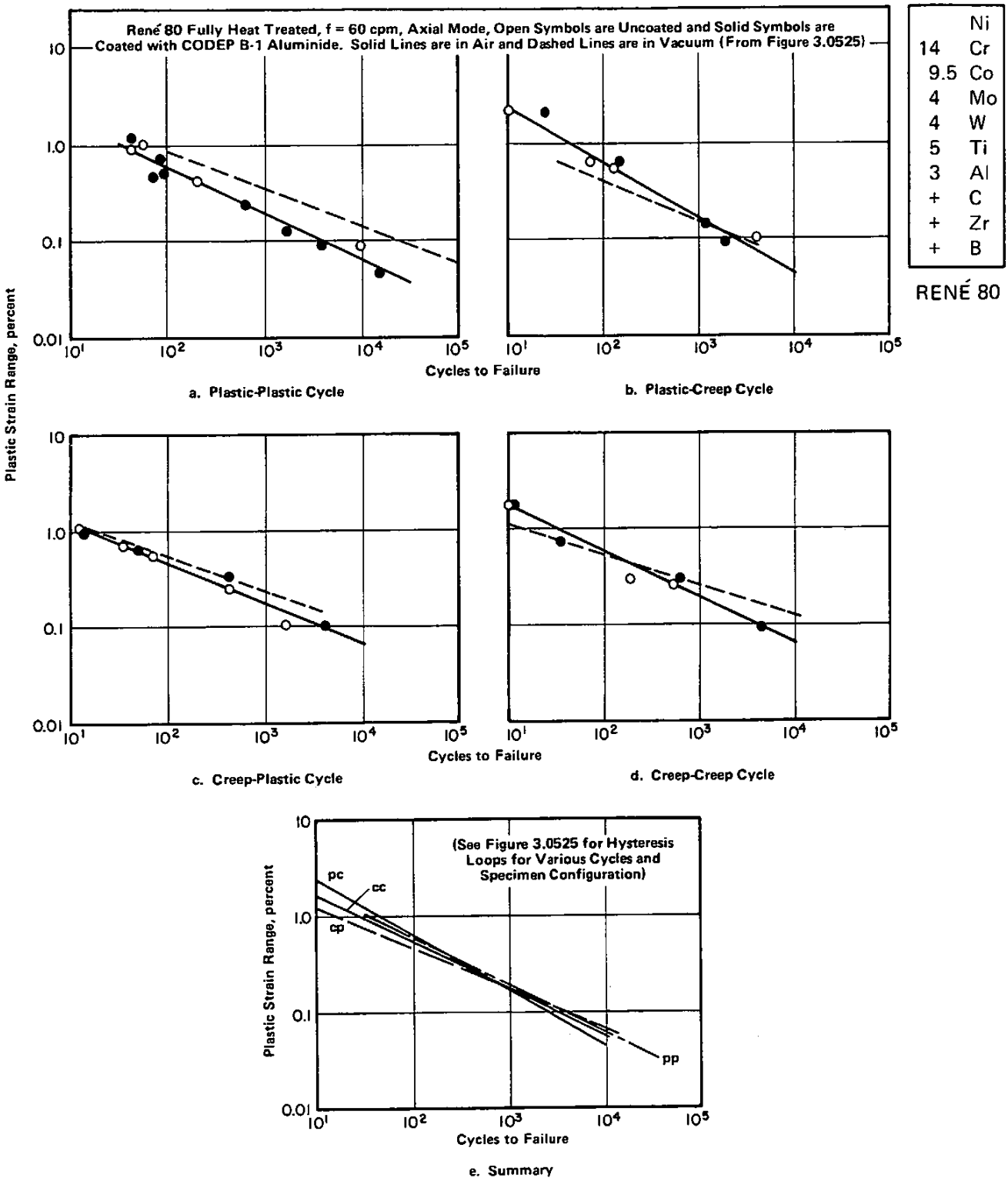

FIGURE 3.0526. EFFECT OF COMBINED PLASTIC AND CREEP-STRAIN CYCLES ON LOW CYCLE FATIGUE LIFE AT 1832 F IN AIR (29)

	Ni
14	Cr
9.5	Co
4	Mo
4	W
5	Ti
3	Al
+	C
+	Zr
+	B

RENÉ 80

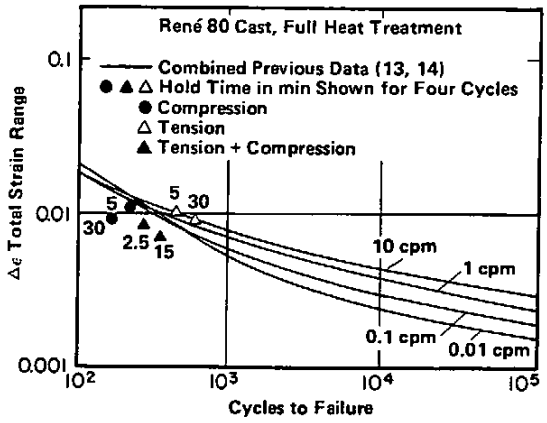

FIGURE 3.0527. COMPARISON OF HOLD TIME EXPERIMENTS WITH FREQUENCY MODIFIED FATIGUE EQUATION REPRESENTATION OF CONTINUOUS CYCLING EXPERIMENTS AT 1600 F (12)

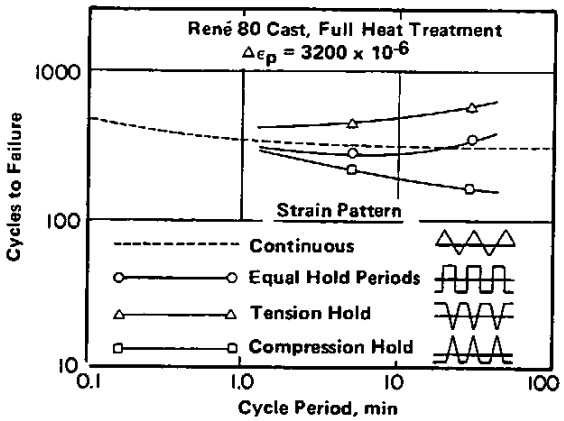

FIGURE 3.0528. EFFECT OF HOLD PERIOD AND WAVE SHAPE ON LOW CYCLE FATIGUE LIFE AT 1600 F (12)

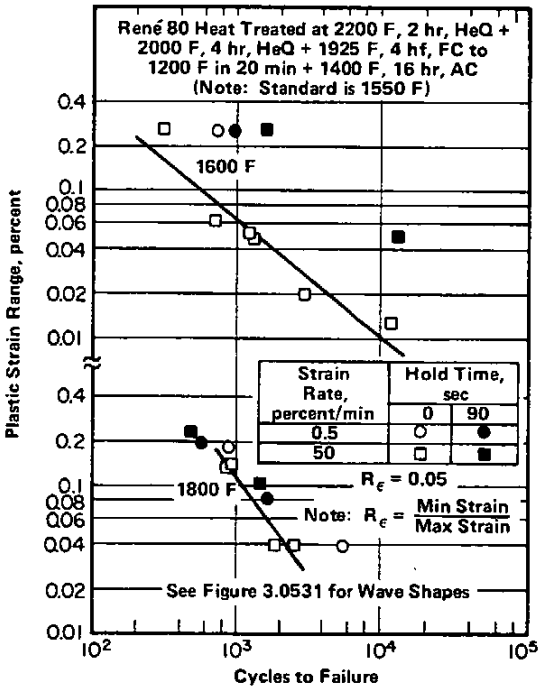

FIGURE 3.0529. EFFECT OF STRAIN RATE AND HOLD TIME ON LOW CYCLE FATIGUE LIFE AT 1600 AND 1800 F (23)

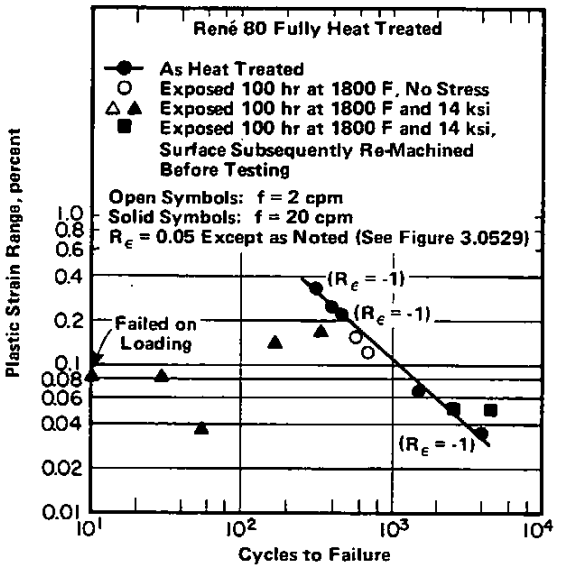

FIGURE 3.0530. EFFECT OF PRIOR AIR EXPOSURE AND CYCLE FREQUENCY ON LOW CYCLE FATIGUE LIFE AT 1600 F (30)

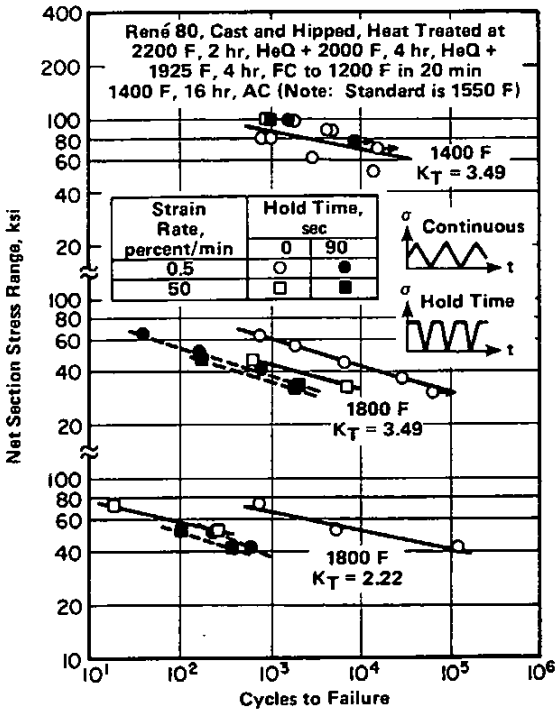

FIGURE 3.0531. EFFECT OF STRAIN RATE AND HOLD TIME ON LOW CYCLE FATIGUE LIFE OF NOTCHED SPECIMENS AT 1400 AND 1800 F (30)

Alloy	René 80	
Condition[a]	Fully Heat Treated – Class A – Hardness R_C 42	
No. of Thermal Cycles to Initiate First Crack	0.025-inch Edge	0.040-inch Edge
Thermal Cycle[b]		
2065/675 F	50	150
1990/600 F	100	100
1915/525 F	125	>500

(a) C50TF28, Class A: 2200 F + 2000 F + 1925 F + 1550 F.
(b) Dwelled for 3 minutes in each bed at the Fluidized Bed Thermal Fatigue Test Facility at IITRI.

TABLE 3.0541. THERMAL CYCLES REQUIRED TO INITIATE FIRST CRACK IN EACH EDGE OF DOUBLE EDGE WEDGE SPECIMEN IN FLUIDIZED BED TESTING (6,11,18)

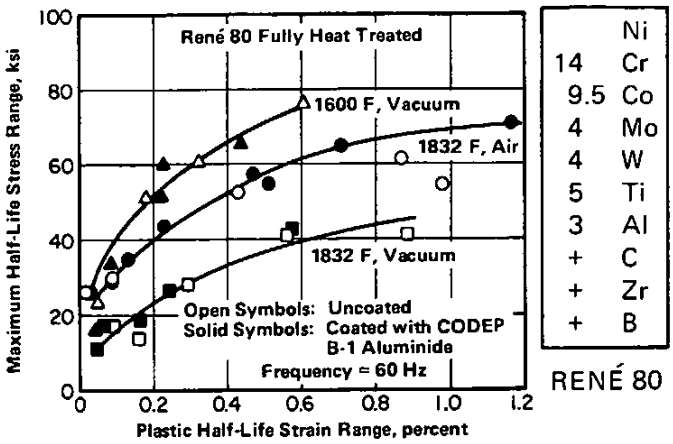

FIGURE 3.0532. CYCLIC STRESS-STRAIN CURVES AT 1600 AND 1832 F IN AIR AND VACUUM (27,29)

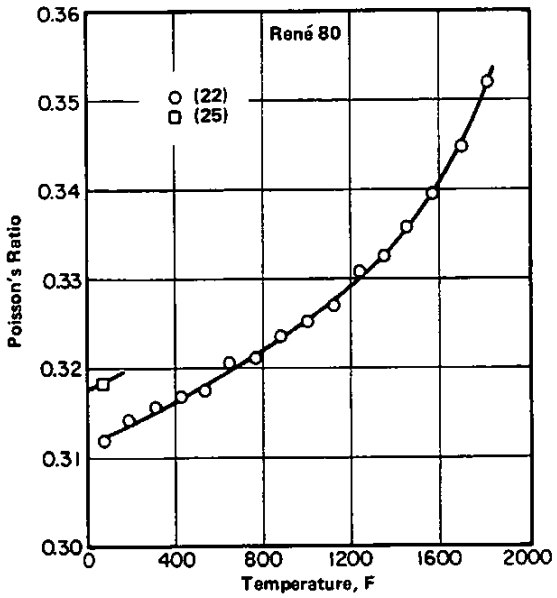

FIGURE 3.061. POISSON'S RATIO (22,25)

	Ni
14	Cr
9.5	Co
4	Mo
4	W
5	Ti
3	Al
+	C
+	Zr
+	B

RENÉ 80

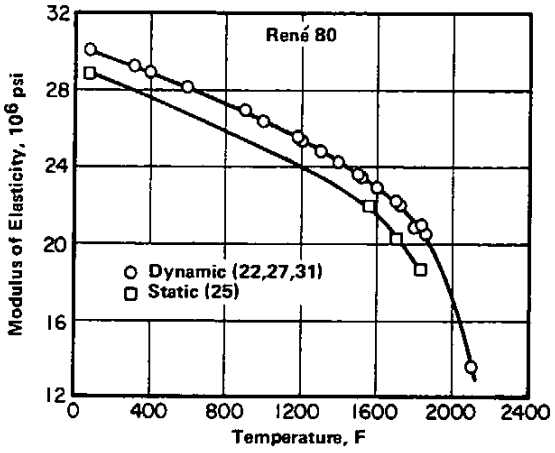

FIGURE 3.062. MODULUS OF ELASTICITY (22,25,27,31)

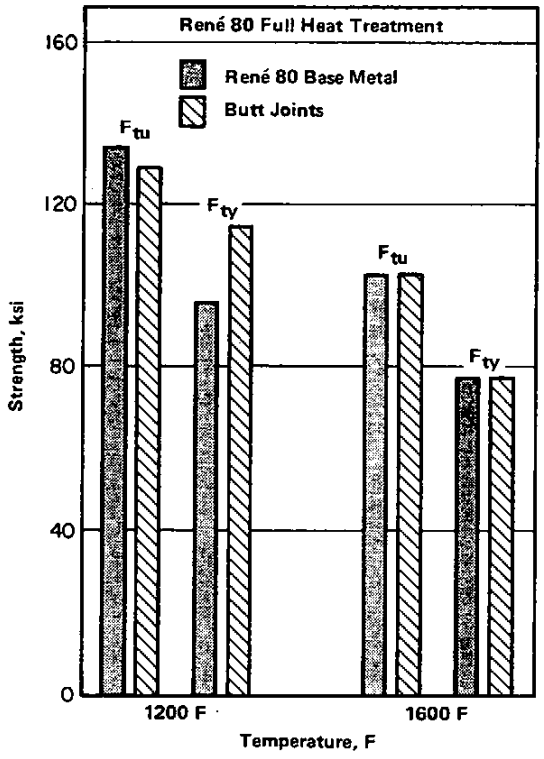

FIGURE 4.032. TENSILE PROPERTIES AT ELEVATED TEMPERATURES OF ACTIVATED DIFFUSION BONDED BUTT JOINTS VERSUS BASE METAL (9)

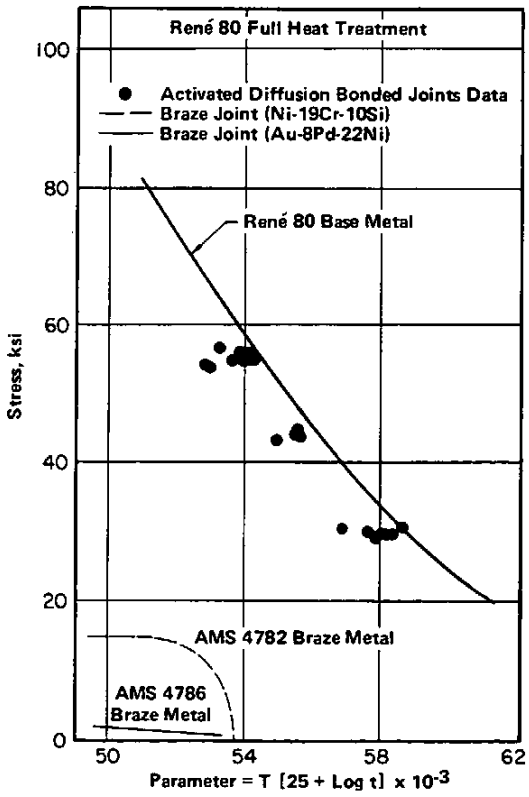

FIGURE 4.033. STRESS RUPTURE STRENGTH OF ACTIVATED DIFFUSION BONDED BUTT JOINTS VERSUS BRAZED JOINTS VERSUS BASE BASE METAL (9)

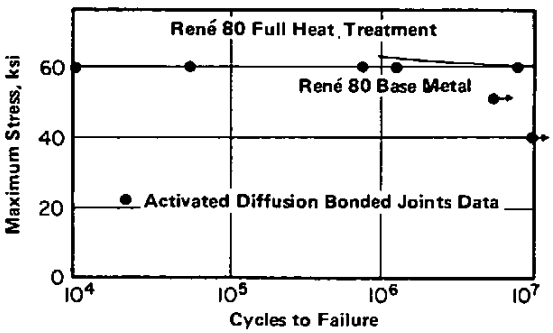

FIGURE 4.034. HIGH CYCLE FATIGUE STRENGTH OF ACTIVATED DIFFUSION BONDED BUTT JOINTS VERSUS BASE METAL AT 1400 F (9)